




# Synthesis and Biological Activity of Novel Zinc-Itraconazole Complexes in Protozoan Parasites and *Sporothrix* spp.

Jose Aleixo de Azevedo-França,<sup>a</sup> Renato Granado,<sup>b</sup> Sara Teixeira de Macedo Silva,<sup>c</sup> Gabrielle dos Santos-Silva,<sup>c,d</sup> Sandra Scapin,<sup>b</sup> Luana P. Borba-Santos,<sup>e</sup> Sonia Rozental,<sup>e</sup> Wanderley de Souza,<sup>c</sup> Érica S. Martins-Duarte,<sup>f</sup> Emile Barrias,<sup>b</sup>  Juliany Cola Fernandes Rodrigues,<sup>c,d</sup> Maribel Navarro<sup>a,b</sup>

<sup>a</sup>Departamento de Química, ICE, Universidade Federal de Juiz de Fora, Juiz de Fora, Brazil

<sup>b</sup>Diretoria de Metrologia Aplicada a Ciências da Vida, Instituto Nacional de Metrologia, Qualidade e Tecnologia, INMETRO, Xerem, Brazil

<sup>c</sup>Laboratório de Ultraestrutura Celular Hertha Meyer, Instituto de Biofísica Carlos Chagas Filho, Universidade Federal do Rio de Janeiro, Rio de Janeiro, Brazil

<sup>d</sup>Núcleo Multidisciplinar de Pesquisa em Biologia, NUMPEX-Bio, Campus UFRJ-Duque de Caxias prof. Geraldo Cidade, Universidade Federal do Rio de Janeiro, Rio de Janeiro, Brazil

<sup>e</sup>Laboratório de Biologia Celular de Fungos, Instituto de Biofísica Carlos Chagas Filho, Universidade Federal do Rio de Janeiro, Rio de Janeiro, Brazil

<sup>f</sup>Departamento de Parasitologia, Instituto de Ciências Biológicas, Universidade Federal de Minas Gerais, Minas Gerais, Brazil

**ABSTRACT** The new complexes Zn(ITZ)<sub>2</sub>Cl<sub>2</sub> (1) and Zn(ITZ)<sub>2</sub>(OH)<sub>2</sub> (2) were synthesized by a reaction of itraconazole with their respective zinc salts under reflux. These Zn-ITZ complexes were characterized by elemental analyses, molar conductivity, mass spectrometry, <sup>1</sup>H and <sup>13</sup>C{<sup>1</sup>H} nuclear magnetic resonance, and UV-vis and infrared spectroscopies. The antiparasitic and antifungal activity of Zn-ITZ complexes was evaluated against three protozoans of medical importance, namely, *Leishmania amazonensis*, *Trypanosoma cruzi*, and *Toxoplasma gondii*, and two fungi, namely, *Sporothrix brasiliensis* and *Sporothrix schenckii*. The Zn-ITZ complexes exhibited a broad spectrum of action, with antiparasitic and antifungal activity in low concentrations. The strategy of combining zinc with ITZ was efficient to enhance ITZ activity since Zn-ITZ-complexes were more active than the azole alone. This study opens perspectives for future applications of these Zn-ITZ complexes in the treatment of parasitic diseases and sporotrichosis.

**KEYWORDS** itraconazole, zinc, *Trypanosoma cruzi*, *Leishmania amazonensis*, *Toxoplasma gondii*, *Sporothrix* spp.

There is an urgent need to discover and develop new and better compounds and therapeutic alternatives to treat parasitic diseases and fungal infections since the ones used in clinics are far from ideal. Well-designed metallodrugs could be candidates to attack these pathogenic agents. Indeed, many transition metal (Pt, Au, Ag, and Zn) complexes have been approved as drugs to successfully treat human diseases, such as cancer, arthritis, ulcers, and microbial illness; some of them are already in clinical trials (1–3). In the last decade, we have been designing potential metallodrugs, using the concept of metal-drug synergism to demonstrate the suitability for metal-based drug discovery purposes by incorporating a metal atom into the structure of clinical drugs to improve their efficacy (4–8).

In previous work, the organic compounds clotrimazole and ketoconazole, from the family of azole derivatives, were coordinated to metals such as Au, Pt, Os, Cu, and Ru to synthesize new metallodrugs, which are more active against protozoan diseases (9) and sporotrichosis agents than the azole drug itself (10, 11). Although transition metal complexes have demonstrated excellent activity and promising results, few zinc-based drugs have been investigated in the development of chemotherapeutic agents effective against parasites (11) or fungi (12–14).

**Citation** Azevedo-França JAD, Granado R, de Macedo Silva ST, Santos-Silva GD, Scapin S, Borba-Santos LP, Rozental S, de Souza W, Martins-Duarte ÉS, Barrias E, Rodrigues JCF, Navarro M. 2020. Synthesis and biological activity of novel zinc-itraconazole complexes in protozoan parasites and *Sporothrix* spp. *Antimicrob Agents Chemother* 64:e01980-19. <https://doi.org/10.1128/AAC.01980-19>.

**Copyright** © 2020 American Society for Microbiology. All Rights Reserved.

Address correspondence to Juliany Cola Fernandes Rodrigues, [juliany.rodrigues@xerem.ufrj.br](mailto:juliany.rodrigues@xerem.ufrj.br), or Maribel Navarro, [maribel.navarro@ufjf.edu.br](mailto:maribel.navarro@ufjf.edu.br).

**Received** 30 September 2019

**Returned for modification** 18 December 2019

**Accepted** 23 February 2020

**Accepted manuscript posted online** 9 March 2020

**Published** 21 April 2020

Combining itraconazole (ITZ), a well-known antimycotic drug with zinc, which is a fairly inexpensive metal and is endogenous and nontoxic, could result in the production of Zn(II)-triazole complexes that would be great alternatives to antiparasitic and antifungal agents. Notably, Zn salts have also demonstrated great activity against diseases, such as acute cutaneous leishmaniasis, attention deficit hyperactivity disorder (ADHD), and Wilson's disease (15–18).

In Brazil, there are some diseases that are neglected by public health policies and pharmaceutical companies and that affect patients from poor socioeconomic backgrounds. Examples are the parasitic diseases caused by *Leishmania* sp., *Trypanosoma cruzi*, and *Toxoplasma gondii* and subcutaneous mycoses, including sporotrichosis. Leishmaniasis, Chagas disease, toxoplasmosis, and sporotrichosis are important diseases affecting a hundred thousand people in all Brazilian states and millions worldwide (19–25). No vaccines are ready for use, and the clinical drugs available to treat them are very limited, require long-term use, and have several side effects; to complicate this further, resistance to some of those medicines have been reported (23, 25–27). In view of this situation, there is an urgent need to development new chemotherapeutic alternatives that are more accessible and efficient.

Sterol biosynthesis is an important pathway for protozoan parasites and fungi since these microorganisms have a special lipid composition that is different from mammalian cells (28). Inhibitors of sterol C14 $\alpha$ -demethylase (CYP51) have been described as effective against protozoan parasites, such as *Leishmania* sp. (28, 29), *Trypanosoma cruzi* (30), and *T. gondii* (31, 32), and they are also used for the treatment of sporotrichosis (19, 20). Itraconazole was shown to be a potent inhibitor of *Leishmania amazonensis* growth, leading to significant ultrastructural alterations that resulted in cell death of the parasites (29). For *T. cruzi*, itraconazole shows significant *in vitro* and *in vivo* results compared with benznidazole or in combination with this compound of choice (30). Besides, in *T. gondii*, itraconazole had potent activity and inhibited parasite proliferation *in vitro* and *in vivo* (31, 32). Thus, itraconazole is a promising molecule that could be used as a molecular scaffold for producing new chemical identities when coordinated with different metals.

In this paper, we report the synthesis, characterization, and biological activity of new Zn-ITZ complexes against three important protozoan parasites, namely, *Leishmania amazonensis*, *Trypanosoma cruzi*, and *Toxoplasma gondii*, and two fungi, namely, *Sporothrix brasiliensis* and *Sporothrix schenckii*. To the best of our knowledge, this is the first report showing the antiparasitic and antifungal effects produced by metal-itraconazole derivatives.

## RESULTS AND DISCUSSION

**Synthesis and characterization of Zn-ITZ complexes.** Two new Zn-ITZ derivatives [Zn(ITZ)<sub>2</sub>Cl<sub>2</sub> (complex 1) and Zn (ITZ)<sub>2</sub>(OH)<sub>2</sub> (complex 2)] were synthesized by a reaction of ITZ with appropriate zinc salt under reflux in methanol, as summarized in the synthesis procedure scheme (Fig. 1). Complex 2 was synthesized under the same conditions of complex 1, and in order to obtain the hydroxyl complex, zinc acetate was used, as it is known to hydrolyze in alcoholic solutions at high temperatures (33, 34). These zinc complexes were all air stable white solids. The infrared (IR) spectra of complexes 1 and 2 showed frequencies associated with the characteristic functional group of itraconazole ligand, such as C=O, C=N, and C=C stretching, which indicates the presence of this ligand in the metal complex structure, although no significant shift for the C=N stretching band was observed.

Analyzing the <sup>1</sup>H-nuclear magnetic resonance (NMR) spectra (Fig. 2), we observed singlets corresponding to H4 (8.69 ppm, 8.31 ppm) and H1 (8.01 ppm and 7.93 ppm) for complexes 1 and 2, respectively. These protons are in the vicinity of nitrogen N5 of the triazole ring where it is believed to cause the coordination to zinc. This can be confirmed by the shifts of these signals compared with the ligand alone. For complex 1, H4 and H1 shifted 0.11 ppm and 0.04 ppm, respectively, while for complex 2 they shifted 0.49 ppm and 0.12 ppm, respectively. According to the literature, zinc acetate

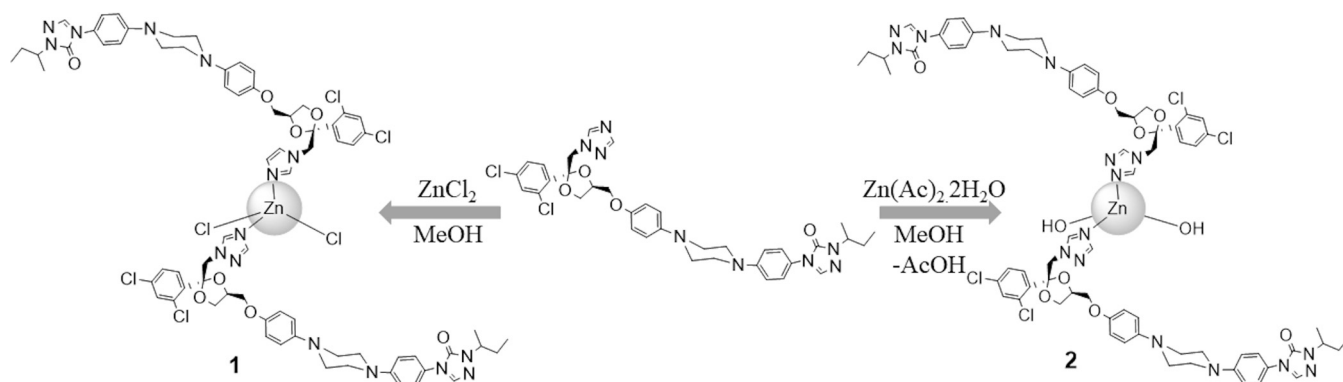


**FIG 1** Scheme of synthetic procedure for obtaining of Zn(ITZ)<sub>2</sub>Cl<sub>2</sub> (1) and Zn(ITZ)<sub>2</sub>(OH)<sub>2</sub> (2).

self-hydrolysis may occur in alcohol solvents in high temperatures to form acetic acid and hydroxyl species that may coordinate to zinc (33, 34). Therefore, as it was expected, for complex 2, no signals corresponding to CH<sub>3</sub>-acetate in <sup>1</sup>H and <sup>13</sup>C NMR spectra were observed, confirming that acetate is not coordinated to zinc.

Moreover, electrospray ionization-tandem mass spectrometry (ESI-MS) spectra of complex 1 and 2 were shown in Fig. 3. For complex 1, peaks corresponding to the molecular ion protonated [Zn(ITZ)<sub>2</sub>Cl<sub>2</sub> + H]<sup>+</sup> = 1,547 *m/z* and the fragment [Zn(ITZ)<sub>2</sub>Cl]<sup>+</sup> = 1,511 *m/z* was observed; for complex 2, ESI-MS spectra showed

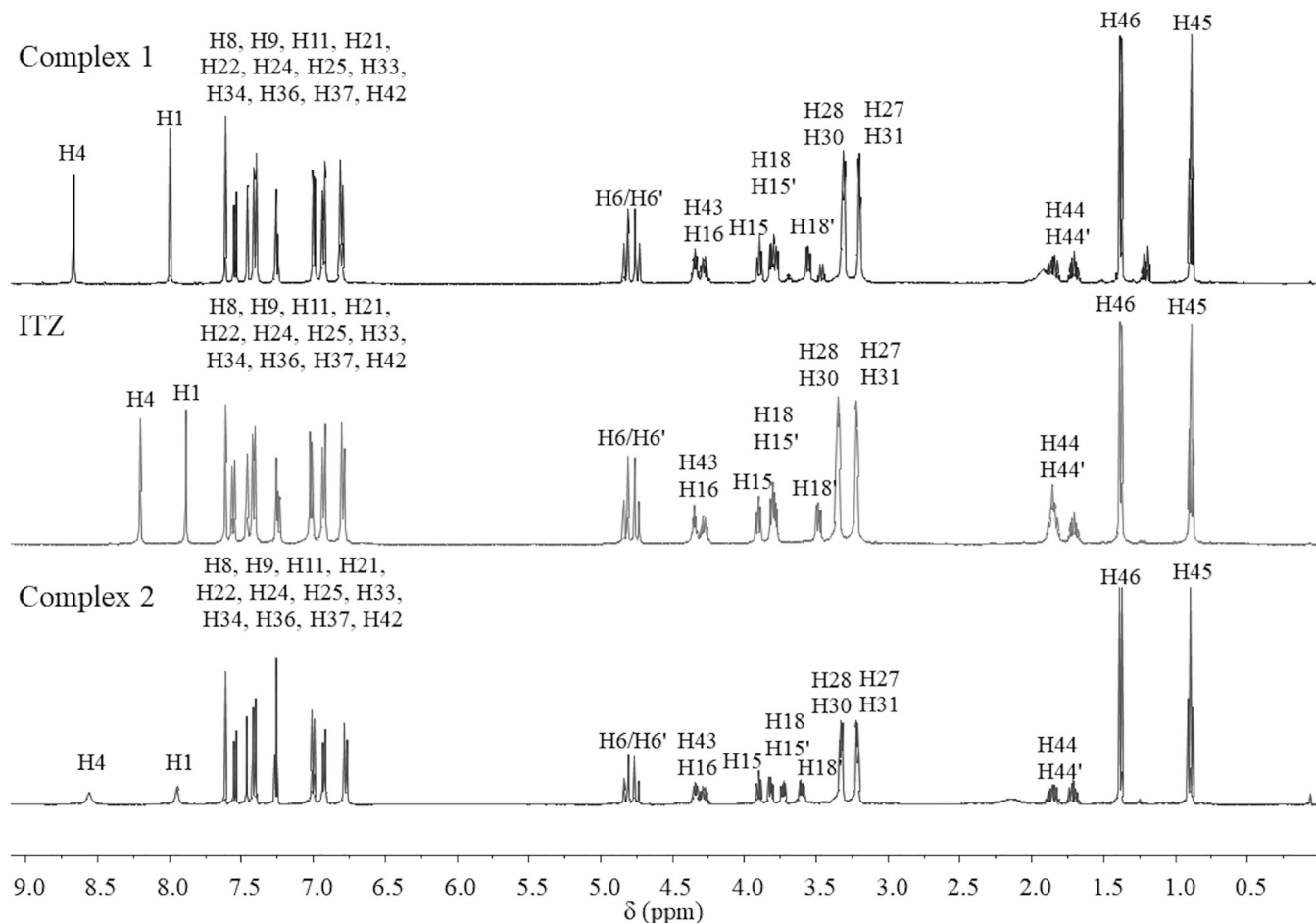


**FIG 2** <sup>1</sup>H NMR spectra of Zn(ITZ)<sub>2</sub>Cl<sub>2</sub> (1), ITZ, and Zn(ITZ)<sub>2</sub>(OH)<sub>2</sub> (2).

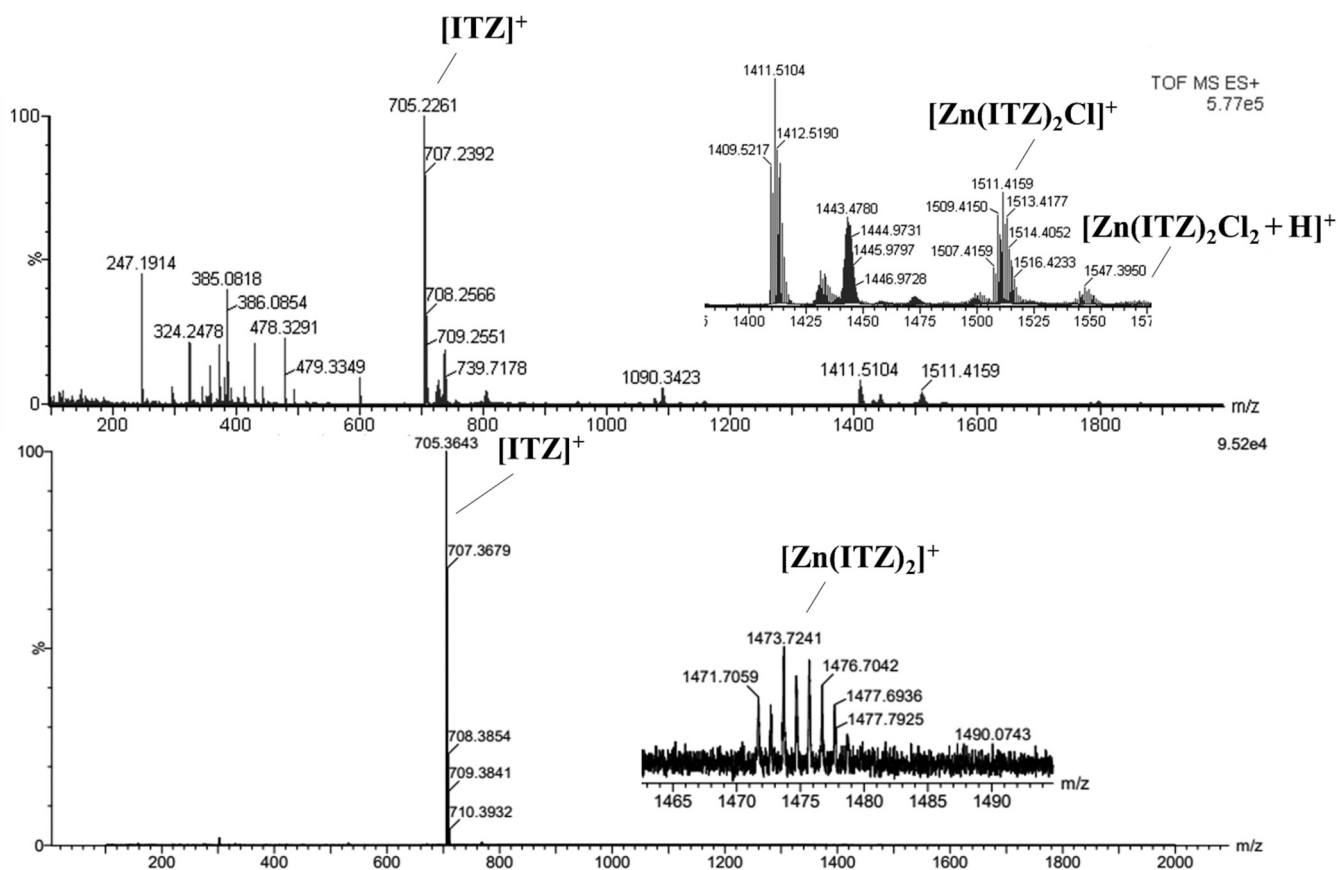


FIG 3 ESI-MS spectra of  $\text{Zn}(\text{ITZ})_2\text{Cl}_2$  (1), ITZ, and  $\text{Zn}(\text{ITZ})_2(\text{OH})_2$  (2).

peaks corresponding to the fragment  $[\text{Zn}(\text{ITZ})_2]^+ = 1473 \text{ m/z}$ , but the molecular ion was not shown. In addition, elemental analyses were all in accordance with the molecular formulas proposed for each complex.

Furthermore, the complexes previously described present a tetrahedral geometry, obeying the 18-electron rule, bearing in mind that the Zn(II) complex electronic configuration is  $d^{10}$  and that they mostly exhibit tetrahedral geometry (35, 36). Also, according to conductivity values, we suggest that these metal complexes show neutral structures, which is in agreement with the data reported (37).

#### Susceptibility and effects on the fine structure of *Leishmania amazonensis*.

Figure 4 shows the effects of ITZ, complex 1, and complex 2 in *L. amazonensis* promastigotes. The effect of ITZ was previously described by our group (29) and confirmed here, resulting in a 50% inhibitory concentration ( $\text{IC}_{50}$ ) value of 44 nM after 72 h of treatment (Fig. 4A). Interestingly, the new Zn-ITZ complexes were more active against promastigotes, resulting in a potent time- and concentration-dependent (time  $\times$  compounds;  $P < 0.0001$ ) inhibition of growth, with  $\text{IC}_{50}$  values of 4 nM and 1.6 nM, for compound 1 and 2, respectively (Fig. 4B and C). These figures also showed that the growth of promastigotes treated with only the zinc salts ( $\text{ZnAc}_2 \cdot 2\text{H}_2\text{O}$  and  $\text{ZnCl}_2$ ) was not significantly altered ( $P > 0.99$ ).

According to the statistical results of the antiproliferative effects in *L. amazonensis* promastigotes (Table 1), an increased efficacy was observed after coordination of ITZ to Zn. A concentration of 0.5  $\mu\text{M}$  was chosen for ITZ, compound 1, and compound 2. The  $P$  values revealed that when ITZ is coordinated to Zn, the growth inhibition begins only with 24 h of exposure to the metallodrugs, which is different from the effects observed for ITZ, where the inhibition was observed only with 72 h of treatment (Table 1). Thus, these analyses suggest a possible synergic effect, also indicating that the Zn-ITZ

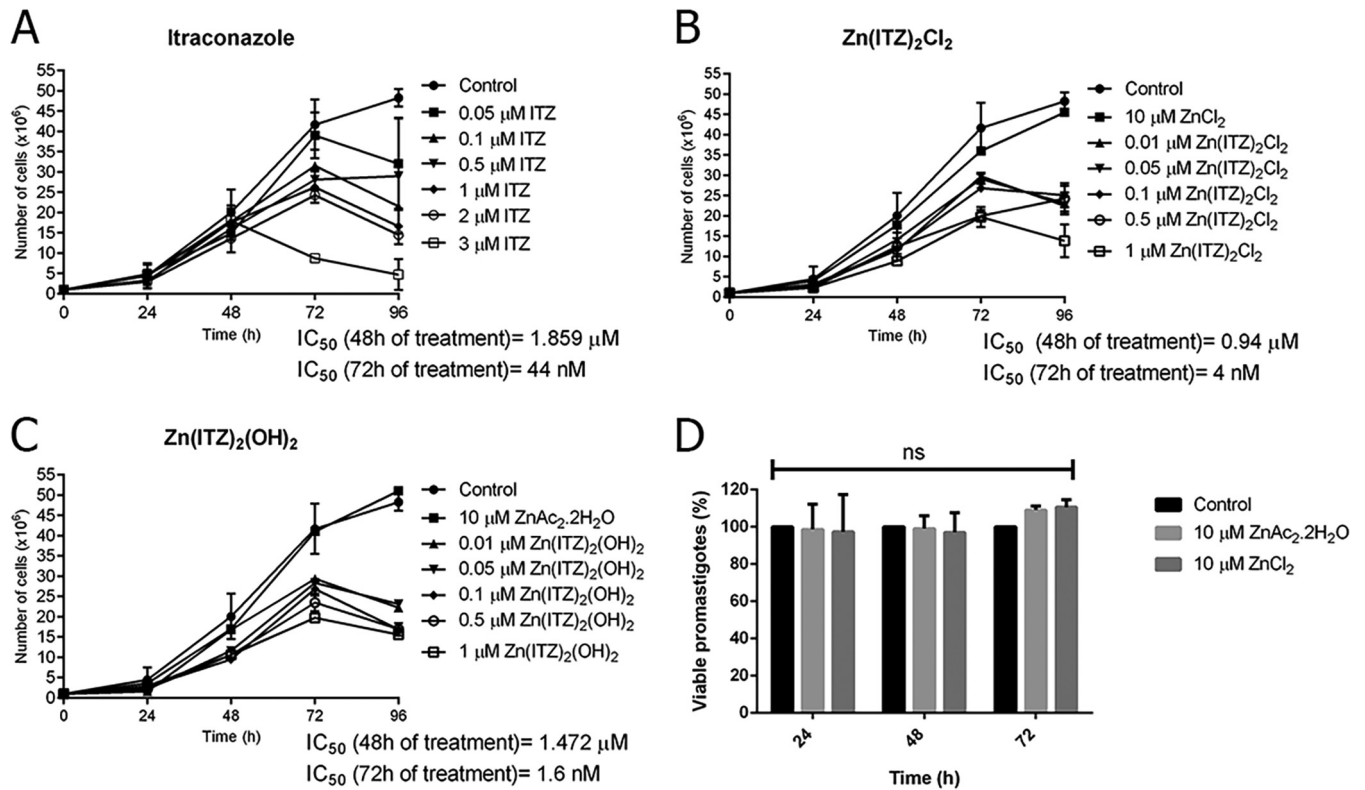


**FIG 4** Antiproliferative effects of itraconazole (ITZ) (A), Zn-ITZ (B, C), and Zn salts (D) on *Leishmania amazonensis* promastigotes. Parasites were treated with different concentrations for 72 h to evaluate growth inhibition. The inhibitors were added after 24 h of growth. The zinc salts ZnAc<sub>2</sub>.2H<sub>2</sub>O and ZnCl<sub>2</sub> used for the synthesis process were not toxic for the promastigotes by counting cells in a Neubauer chamber (B, C) and also by MTS/PMS assay (D). Graphics represent the means and standard deviation of three independent experiments. Two-way repeated measures ANOVA with Dunnett's *post hoc* test was used for statistical analysis. For each treatment group and variable, the following *P* values were obtained: (A) ITZ, *P* = 0.04, *P* < 0.0001 (time), *P* < 0.0001 (interaction); (B) compound 1, *P* = 0.0007, *P* < 0.0001 (time), *P* < 0.0001 (interaction); and (C) compound 2, *P* = 0.0002, *P* < 0.0001 (time), *P* < 0.0001 (interaction). (D) Zinc salts.

complexes are multitarget drugs. Besides, Fig. 4D confirmed that the zinc salts were not toxic for the promastigotes, corroborating with the possibility of a combined effect of the Zn-ITZ complexes.

The Zn-ITZ complexes were much more effective against the intracellular amastigotes, the clinically relevant stage of the parasite; the antiproliferative effects of the treatments were very potent, resulting in  $IC_{50}$  values of 145.38 nM, 0.118 nM, and 33.07 nM for ITZ, compound 1, and compound 2, respectively (Fig. 5). In contrast to the results obtained for promastigotes, where the most potent complex was compound 2, the most potent complex against amastigotes was compound 1. Selectivity indexes (SIs) were calculated using the relation between 50% cytotoxic concentration ( $CC_{50}$ ) and  $IC_{50}$  values obtained after 72 h of treatment, and compound 1 was more selective and tolerable of them, with an SI of 5,084 (Table 2). We also evaluated the zinc salts against RAW264.7 macrophages, trying to observe possible cytotoxic effects against

**TABLE 1** *P* values obtained after statistical analysis by two-way repeated measures ANOVA with Dunnett's *post hoc* test of the antiproliferative studies on *Leishmania amazonensis* promastigotes<sup>a</sup>

Dunnett's multiple-comparison test groups	<i>P</i> values by time of treatment (h)		
	24	48	72
Control vs. 0.05 $\mu$ M ITZ	0.6555 <sup>b</sup>	0.9503 <sup>b</sup>	0.0084
Control vs. 0.05 $\mu$ M Zn(ITZ) <sub>2</sub> Cl <sub>2</sub> (compound 1)	0.0039	<0.0001	<0.0001
Control vs. 0.05 $\mu$ M Zn(ITZ) <sub>2</sub> (OH) <sub>2</sub> (compound 2)	0.0003	<0.0001	<0.0001

<sup>a</sup>Analysis of Fig. 4A to C with 0.05  $\mu$ M of each drug and in all of three times of treatment.

<sup>b</sup>Not significant.

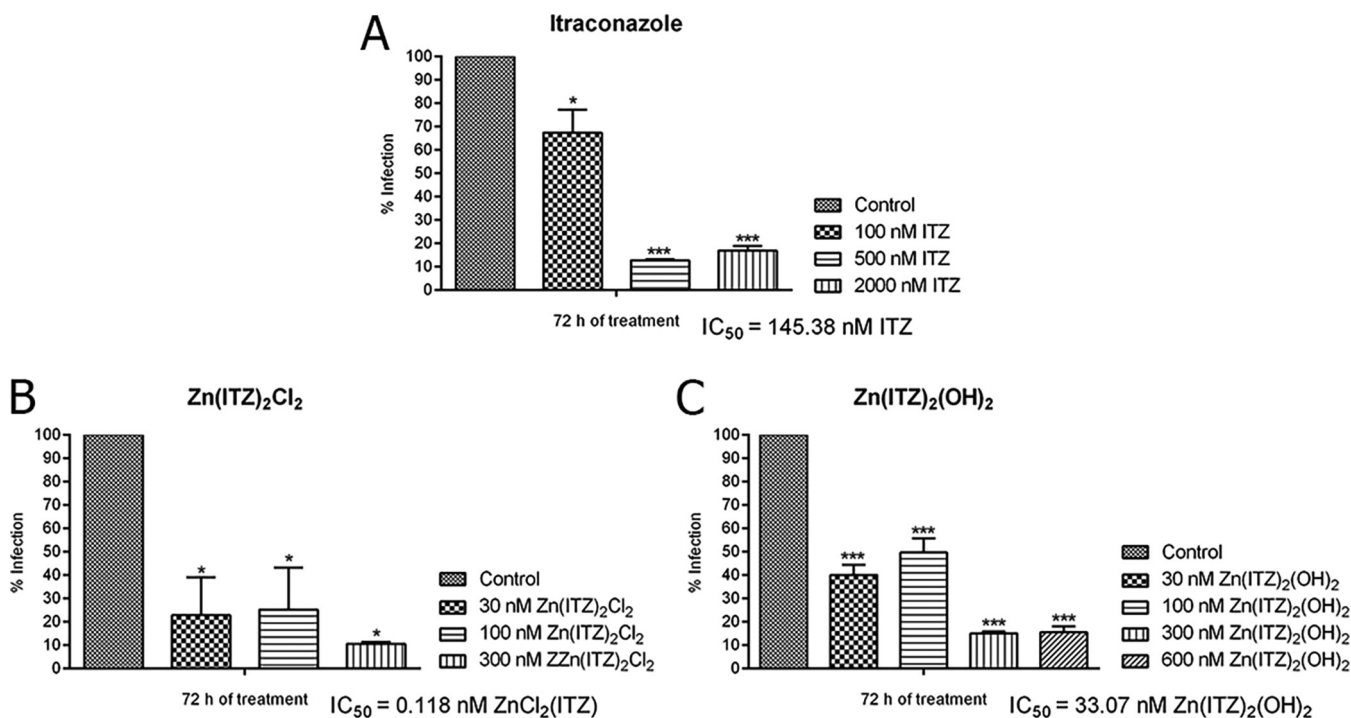


**FIG 5** Antiproliferative effects of itraconazole (ITZ) (A), compound 1 (B), and compound 2 (C) on *Leishmania amazonensis* intracellular amastigotes after 72 h of treatment. Graphics represent the means and standard deviation of three independent experiments. The one-way ANOVA with Bonferroni's *post hoc* test were used for *P* value calculations. Asterisks mean different degrees of significance between treated groups and the control. \**P* < 0.05, \*\**P* < 0.01, and \*\*\**P* < 0.001.

mammalian cells, and the results indicated that they were toxic in concentrations up to 10 μM.

Scanning electron microscopy (SEM) and transmission electron microscopy (TEM) revealed several alterations in *L. amazonensis* promastigotes (Fig. 6 and 7). The effects of ITZ have been described previously (29). By SEM, when promastigotes were treated with 0.5 μM ITZ, compound 1, and compound 2 for 48 h, they appeared rounded and swollen (Fig. 6B to F), sometimes presenting more than two flagella (Fig. 6B, arrowhead). By TEM, several alterations were observed after treatment, such as (i) intense mitochondrial swelling followed by its disorganization (Fig. 7B to F); (ii) presence of lipid bodies (Fig. 7C); and (iii) presence of vacuoles similar to autophagosomes, some of them containing small vesicles and membrane profiles (Fig. 7B to F). Images also indicated a close association between these vacuoles and organelles such as the nucleus (Fig. 7F, arrow).

Morphological and ultrastructural analyses revealed several alterations in the shape of the cell body, membrane structure, and presence of lipid bodies that could indicate possible inhibition of the ergosterol biosynthesis, as we also observed for other C14α-demethylase inhibitors, including itraconazole (28, 29). We also observed the

**TABLE 2** Antiproliferative effects on *Leishmania amazonensis* intracellular amastigotes<sup>a</sup>

Compound	IC <sub>50</sub> of intracellular amastigotes at 72 h (nM)	CC <sub>50</sub> of peritoneal or RAW264.7 macrophages at 72 h (nM)	Selective index (CC <sub>50</sub> /IC <sub>50</sub> )
ITZ	145.38	15,000	103.17
Zn(ITZ) <sub>2</sub> Cl <sub>2</sub> (1)	0.118	600	5,084
Zn(ITZ) <sub>2</sub> (OH) <sub>2</sub> (2)	33.07	800	24.19
ZnCl <sub>2</sub>		>10,000	
ZnAc <sub>2</sub> ·2H <sub>2</sub> O		10,000	

<sup>a</sup>Parasites were treated with different concentrations for 72 h to evaluate the growth inhibition. The inhibitors and zinc salts were added after 24 h of growth.

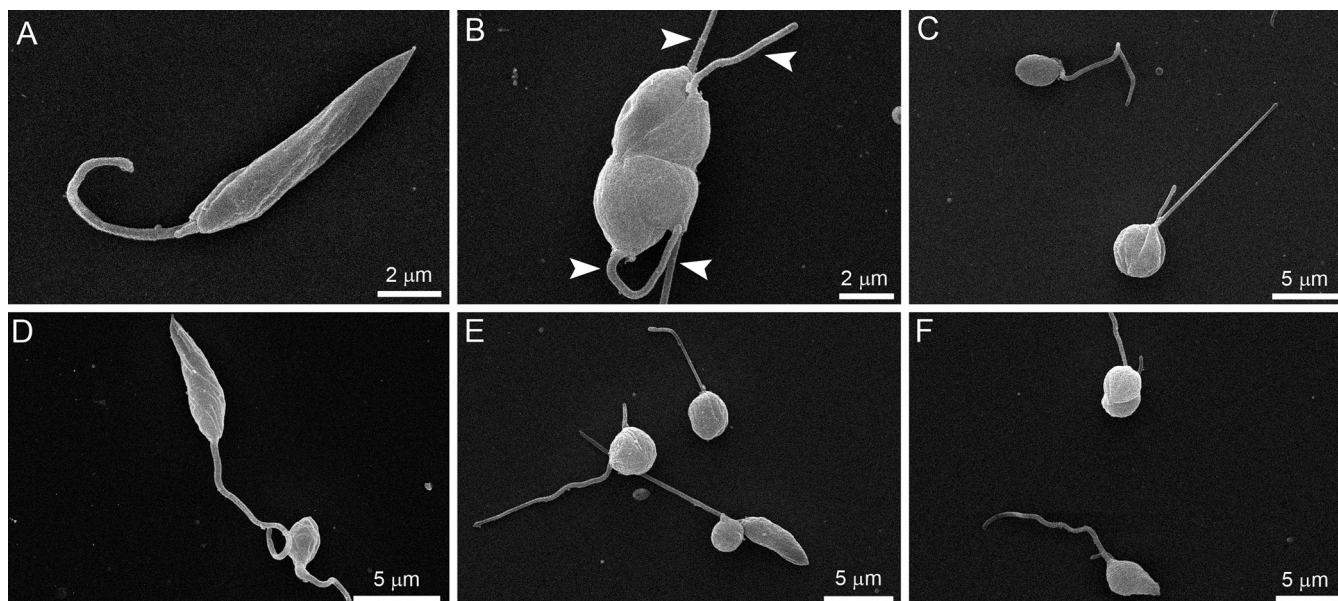


**FIG 6** Scanning electron microscopy of *Leishmania amazonensis* promastigotes. (A) Control parasites after 72 h of growth; (B, C) 0.5  $\mu\text{M}$  itraconazole (ITZ); (D) 0.5  $\mu\text{M}$  compound 1; and (E, F) 0.5  $\mu\text{M}$  compound 2. Treatment induced significant alterations in the shape of cell bodies; the parasites presented swollen and rounded (B–F), some of them with a long flagellum, sometimes with more than two flagella (B, arrowhead).

presence of big vacuoles similar to autophagosomes that could be related with autophagy and an increased activity in the remodeling of abnormal lipids and organelles affected by the treatment. These changes observed in the Fig. 6 and 7 should result in the death of the treated parasites since the number of promastigotes at the culture cells reduced significantly with 96 h of growth (Fig. 4A to C). On the other hand, possible alterations in the chromatin condensation, as we observed in Fig. 4C and D, could be induced by the zinc ion.

**Effect of ITZ and Zn-ITZ complexes against *Toxoplasma gondii*.** In previous work, our group showed that ITZ is highly active against *T. gondii* tachyzoites, inhibiting parasite proliferation, with an  $\text{IC}_{50}$  at a nanomolar range (31). Here, we confirm the activity of ITZ against *T. gondii* (Table 3) but also show that both Zn-ITZ complexes were more effective against *T. gondii* than ITZ. Results in Table 3 show that compound 1 and 2 inhibited *T. gondii* proliferation, with  $\text{IC}_{50}$  lower than that obtained for ITZ; besides, an interesting result was related with the difference of action between the two zinc complexes. While  $\text{Zn}(\text{ITZ})_2\text{Cl}_2$  (compound 1) was more active, presenting an  $\text{IC}_{50}$  of 38.7 nM, which was 5 times lower than ITZ (196.1 nM),  $\text{Zn}(\text{ITZ})_2(\text{OH})_2$  (compound 2) presented an  $\text{IC}_{50}$  of 72.0 nM, which was just 2.7 times lower than ITZ. Furthermore, Zinc-ITZ complexes were also more tolerable for host cells, as both compound 1 and 2 showed an SI higher than that for ITZ. Statistical analysis using a one-way analysis of variance (ANOVA) test confirmed that the differences found in the  $\text{IC}_{50}$  of compounds 1 and 2 compared to ITZ were significant ( $P < 0.01$ ).

**Antiproliferative effects of ITZ and Zn-ITZ complexes against *Trypanosoma cruzi*.** We report the effects of ITZ, complex 1, and complex 2 in *T. cruzi* epimastigotes and intracellular amastigotes. For epimastigotes, after 72 h of treatment, the  $\text{IC}_{50}$  values obtained were 87 nM, 3.31 nM, and 1.3 nM for ITZ, compound 1, and compound 2, respectively, demonstrating that Zn-ITZ complexes are more than 10 times more active against epimastigotes than ITZ (Fig. 8A to C). For intracellular amastigotes, the clinically relevant stage of the parasite, the three compounds were much more active, resulting in  $\text{IC}_{50}$  values of 2.3 nM, 1.14 nM, and 0.91 nM for ITZ, compound 1, and compound 2, respectively, after 96 h of infection (Table 4). As in *L. amazonensis*, compound 2 was more effective than compound 1. Selectivity indexes (SIs) were calculated using the  $\text{CC}_{50}$  and  $\text{IC}_{50}$  values obtained after 72 h of treatment,

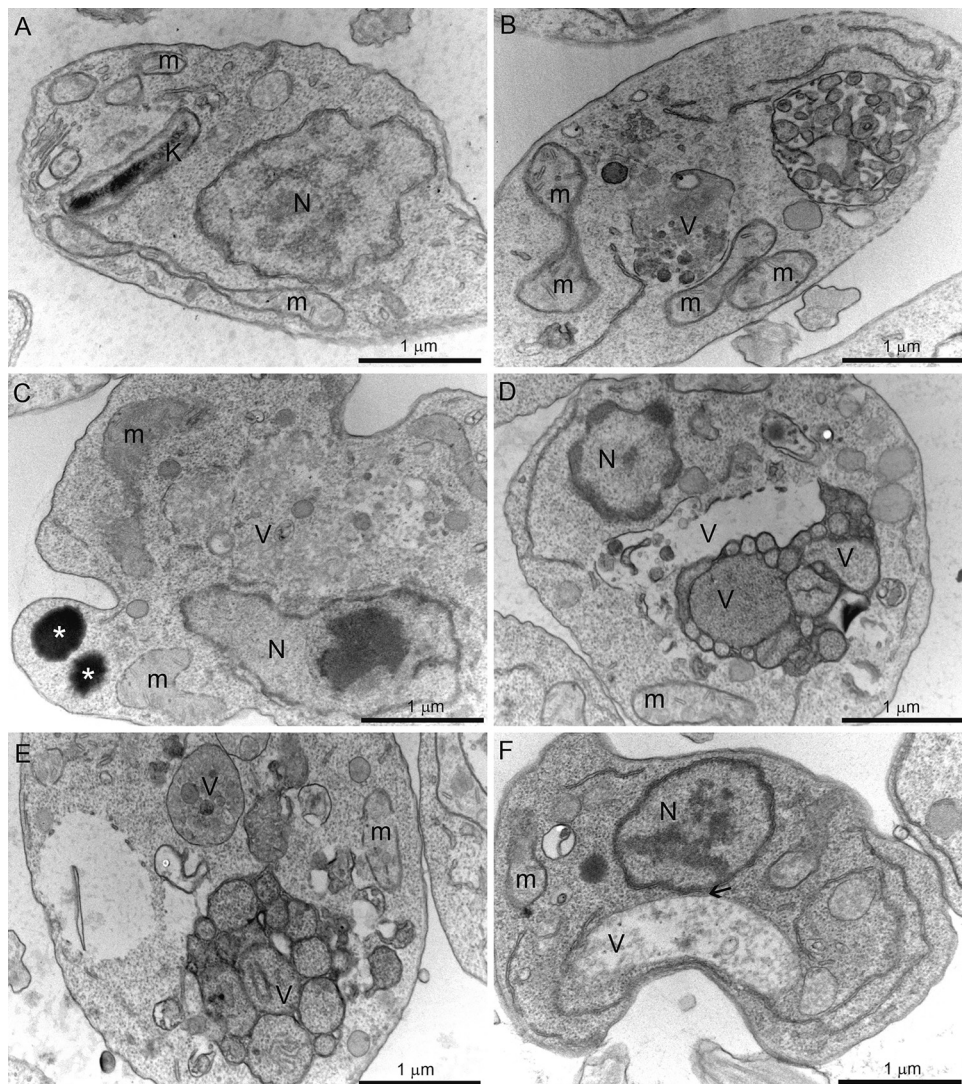


**FIG 7** Transmission electron microscopy of *Leishmania amazonensis* promastigotes control (A) and treated with 0.5 μM itraconazole (ITZ) (B, C), 0.5 μM compound 1 (D, E), or 0.5 μM compound 2 (F) after 72 of treatment. Several alterations were observed, such as intense disorganization and swelling of the mitochondrion (B, C, E), the presence of lipid bodies (C), and the appearance of vacuoles similar to autophagosomes (B–F) close to organelles such as the nucleus (F, arrow). V, vacuole; K, kinetoplast; M, mitochondrion; N, nucleus.

and compound 1 and 2 were more selective and tolerable than ITZ, with SIs of 323.6 and 555.38, respectively (Table 4).

Scanning electron microscopy (SEM) (Fig. 9) and transmission electron microscopy (TEM) (Fig. 10) revealed several alterations in *Trypanosoma cruzi* epimastigotes (Fig. 9 and 10). By SEM, epimastigotes treated with IC<sub>50</sub> of ITZ (Fig. 9B), compound 1 (Fig. 9E),

**TABLE 3** Anti-*Toxoplasma gondii* activity and cytotoxicity against HFF cells of ITZ and Zn-ITZ complexes<sup>a</sup>

Compound	IC <sub>50</sub> (nM) by treatment time (h)		Cytotoxicity values	
	72	96	CC <sub>50</sub> (nM)	SI
ITZ	162.3 ± 43.6	196.1 ± 65.7	>5,000	>25.5
Zn(ITZ) <sub>2</sub> Cl <sub>2</sub> (1)	37.2 ± 12.4*	38.7 ± 9.1*	>5,000	>129.2
Zn(ITZ) <sub>2</sub> (OH) <sub>2</sub> (2)	60.0 ± 15.22*	72.0 ± 33.8*	>5,000	>69.4

<sup>a</sup>Results are expressed as mean ± standard deviation of three different experiments. \*, P value is <0.01 compared with ITZ IC<sub>50</sub>.



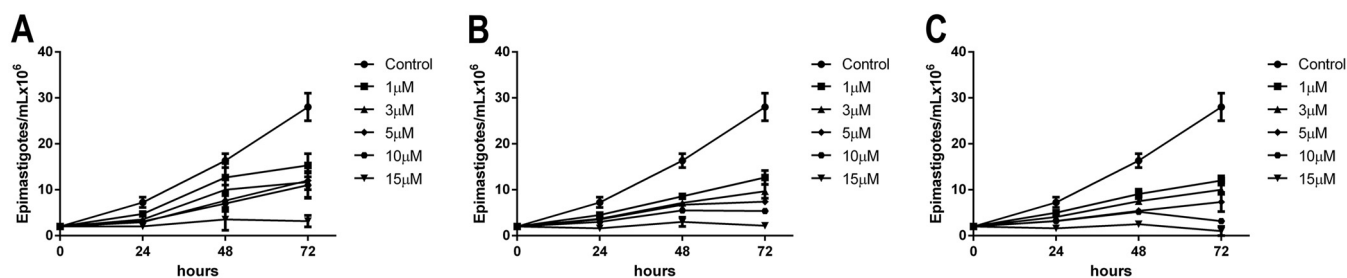


**FIG 8** Antiproliferative effects of itraconazole (ITZ) (A), compound 1 (B), and compound 2 (C) on *Trypanosoma cruzi* epimastigotes. Parasites were treated with different concentrations for 72 h to evaluate the growth inhibition. Graphics represent the means and standard deviation of three independent experiments.

and compound 2 (Fig. 9C and D) for 48 h appeared rounded (Fig. 9B, D to E) compared with the control (Fig. 9A). About 30% of epimastigotes treated for 48 h with compound 2 presented multiple flagella (Fig. 9C, arrow). The same pattern was also observed for the treatment with IC<sub>50</sub> of ITZ; however, the manifestation of this phenomenon was less frequent (Fig. 9B, arrow). By TEM, several alterations were observed after treatment (Fig. 10), such as (i) Golgi complex disorganization (Fig. 10B, GC) and the presence of vacuoles similar to autophagosomes with small vesicles inside (Fig. 10, arrow); (ii) intense mitochondrial swelling (M) followed by its disorganization (Fig. 10C, arrow); (iii) the presence of multiple flagella (Fig. 10C, F); (iv) the presence of a disorganized kinetoplast (Fig. 10D, K); and (v) a membrane flagella detachment (Fig. 10E, F) compared with the control (Fig. 10A).

**Antifungal effect of Zn-ITZ complexes against *Sporothrix brasiliensis* and *S. schenckii*.** The *in vitro* susceptibility of *S. brasiliensis* and *S. schenckii* yeasts to compounds 1 and 2 was established by determining MIC and minimal fungicidal concentration (MFC) values, and these values were compared with those of ITZ, ZnCl<sub>2</sub>, and ZnAc<sub>2</sub>·2H<sub>2</sub>O (Table 5). Concentrations of Zn-ITZ complexes required to inhibit fungal growth (MIC) were lower than those of ITZ alone for both species, but compound 1 was found to be more active than compound 2 (Table 5). Compound 1 was also the only tested compound able to kill *S. brasiliensis* and *S. schenckii* at concentrations lower than 20 μM (Table 5). The zinc salts were not able to inhibit or kill *S. brasiliensis* and *S. schenckii* at concentrations up to 20 μM (Table 5). No hemolytic effect toward red blood cells was observed for compound 1 at concentrations up to 1,000 μM, while the 50% hemolysis (HA<sub>50</sub>) value of ITZ was 700 μM (Table 5). The selectivity indexes (SIs) revealed that compound 1 was at least 12,500 times more selective toward *Sporothrix* spp. than it was toward red blood cells (Table 5).

The significant efficacies displayed for the Zn-ITZ complexes against the protozoa and fungi demonstrated that these metal complexes might act as multitarget drugs, where itraconazole inhibits sterol 14-α demethylases of the parasitic cytochrome P-450 (38), while zinc (an essential trace element for human survival; it has clinical relevance) could act by modes of action already reported (39, 40) or by new ones, which we plan to evaluate in future studies. Thus, we plan to determine in the mechanisms of action

**TABLE 4** Anti-*Trypanosoma cruzi* activity and cytotoxicity against LLC-MK<sub>2</sub> cells of ITZ and Zn-ITZ complexes<sup>a</sup>

Compound	IC <sub>50</sub> (nM) of:		Cytotoxicity values	
	Epimastigotes <sup>b</sup>	Intracellular amastigotes <sup>c</sup>	CC <sub>50</sub> (nM)	SI
ITZ	87.0 ± 11.3	2.3 ± 0.87	152.5	66.3
Zn(ITZ) <sub>2</sub> Cl <sub>2</sub> (1)	3.31 ± 2.57*	1.14 ± 0.91*	368.91	323.6
Zn(ITZ) <sub>2</sub> (OH) <sub>2</sub> (2)	1.3 ± 1.8*	0.91 ± 0.76*	505.4	555.38

<sup>a</sup>Results are expressed as mean ± standard deviation of three different experiments. \*, P value is <0.01 compared with ITZ IC<sub>50</sub>.

<sup>b</sup>Epimastigotes were treated with different concentrations for 48 h to evaluate the growth inhibition.

<sup>c</sup>Amastigotes were treated for 72 h after 24 h of infection.

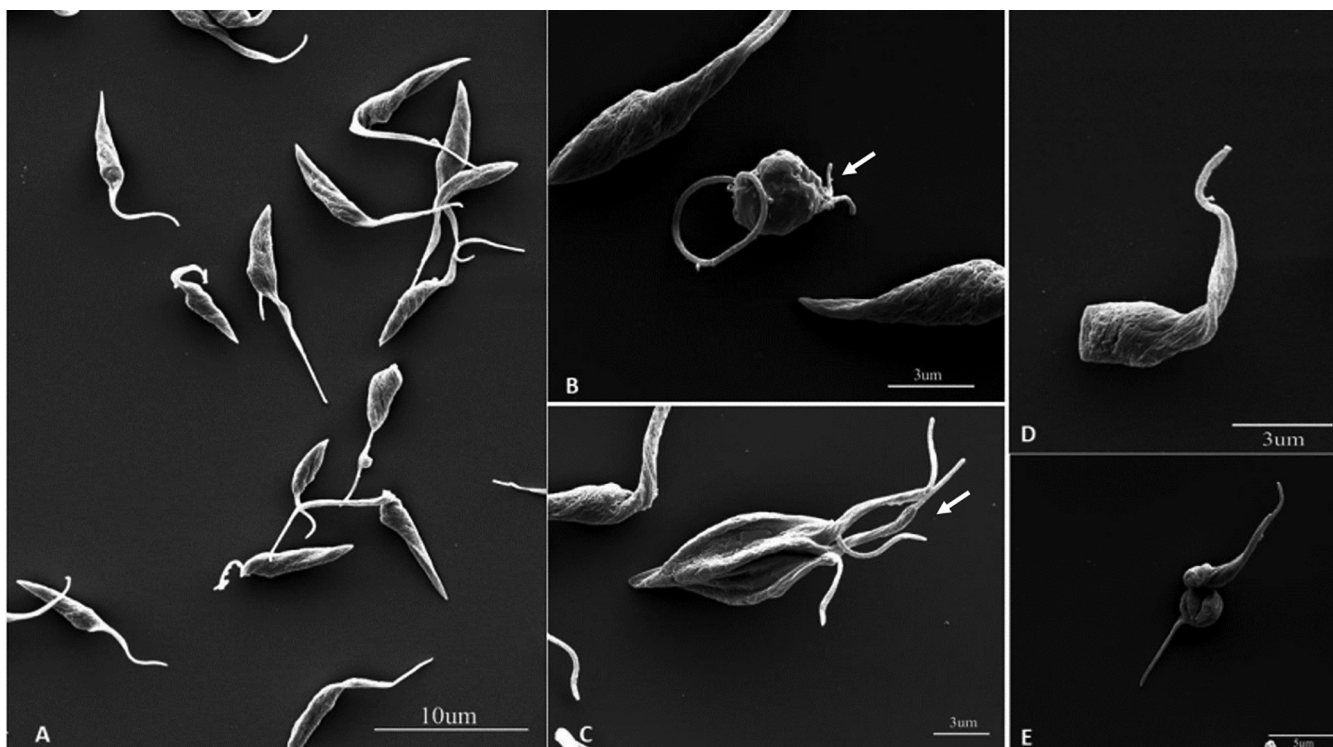


**FIG 9** Scanning electron microscopy of *Trypanosoma cruzi* epimastigotes treated with  $IC_{50}$  of ITZ, compound 1, and compound 2 for 72 h. Epimastigote cultures grown in the absence (A) or presence of ITZ (B), compound 2 (C, D) or compound 1 (E). After 72 h of treatment, epimastigotes were collected, washed, and processed for SEM. Control parasites presented a feature morphology with an elongate body and a flagellum emerging from the anterior region (A). Parasites have body contorted and rounded cell (B, D, E) and multiple flagella (B, C, arrow).

in future studies to better understand the contribution of both parts of these new chemical identities.

**Conclusions.** In conclusion, the newly synthesized complexes  $Zn(ITZ)_2Cl_2$  and  $Zn(ITZ)_2(OH)_2$  exhibited a broad spectrum of action, with antiparasitic and antifungal activity at low concentrations. In *L. amazonensis* and *T. cruzi*, Zn-ITZ derivatives resulted in several ultrastructural alterations that could lead the parasites to cell death, confirming the potent effect of the new chemical identities. The strategy of combining zinc with ITZ was efficient to enhance ITZ activity because Zn-ITZ complexes were more active than azoles. Interestingly,  $Zn(ITZ)_2Cl_2$  (1) had better results against *L. amazonensis*, *T. gondii*, *S. brasiliensis*, and *S. schenckii* than  $Zn(ITZ)_2(OH)_2$ . Thus, this study opens perspectives for future applications of these Zn-ITZ complexes in the treatment of parasitic disease and sporotrichosis.

## MATERIALS AND METHODS

**Chemical syntheses.** Solvents for the reaction were purchased from Tedia. Zinc acetate dihydrate and zinc chloride were purchased from Vetec (Rio de Janeiro, Brazil). Itraconazole (2-butan-2-yl-4-[4-[4-[4-[[[(2"R,"4"S")-2-(2,4-dichlorophenyl)-2-(1,2,3-triazol-1-ylmethyl)-1,3-dioxolan-4-yl]methoxy]phenyl]piperazin-1-yl]phenyl]-1,2,4-triazol-3-one) was obtained from Calendula Pharmaceutic (São Carlos, Brazil). All commercial reagents were used without further purification. The syntheses were all carried out under room atmosphere conditions. Zn-ITZ complexes were characterized using the following spectroscopic and analytical techniques; the IR spectra were obtained with a Shimadzu spectrometer in the 4,000- to 400- $cm^{-1}$  region. The electrospray ionization-tandem mass spectrometry (ESI-MS) spectra were recorded on a Water Synapt high-definition mass spectrometry (HDMS) time of flight (TOF) instrument with a hybrid quadrupole analyzer, using methanol as a solvent. The elemental composition of the metal complexes was determined using a Perkin Elmer 2400 CHNS/O Series II microanalyzer. Conductivity values were obtained using a Meter Lab CDM2300 instrument. NMR experiments were performed at 298 K on a Bruker Avance III HD 500 spectrometer, 9.4 T, and observing  $^1H$  at 500 and  $^{13}C\{^1H\}$  at 125. The NMR spectra were recorded in  $CDCl_3$  solutions with trimethylsilyl (TMS) ( $^1H$  and  $^{13}C\{^1H\}$ ).

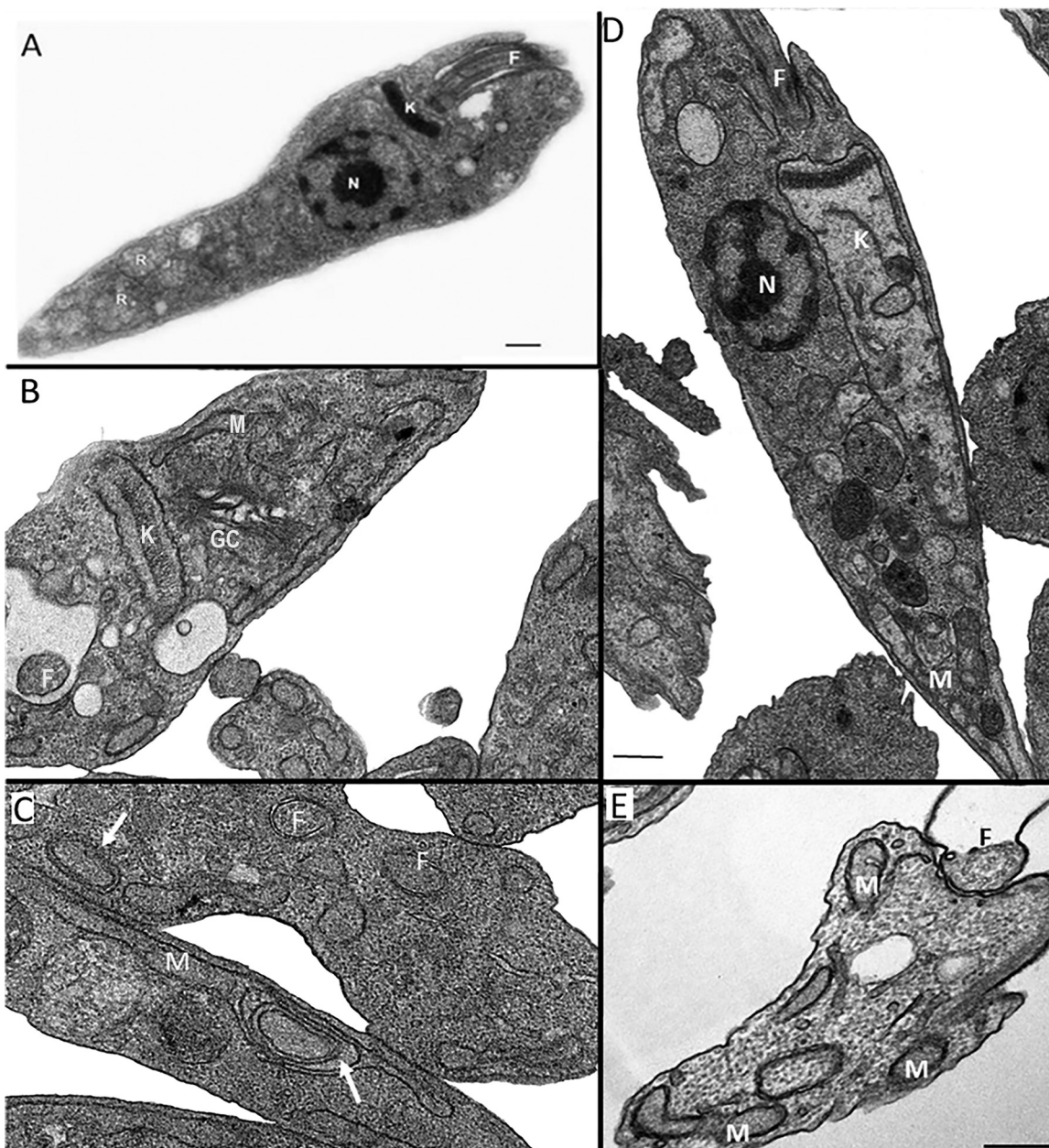


**FIG 10** Transmission electron microscopy of *Trypanosoma cruzi* epimastigotes treated with ITZ and compound 2 for 72 h. (A) Control without treatment presents all structures preserved. (B) 100 nM ITZ; (C–E) 5 nM compound 2. Several alterations were observed, such as Golgi complex disorganization (B, GC), vacuoles similar to autophagosomes (B, C, arrow), intense disorganization and swelling of the mitochondrion (C, D, arrow), kinetoplast disorganization and swelling (D), and a flagellar membrane detachment (E). F, flagellum; GC, Golgi complex; M, mitochondrion; N, nucleus; k, kinetoplast. Bars = 0.5  $\mu\text{m}$ .

Zn(ITZ)<sub>2</sub>Cl<sub>2</sub>·2H<sub>2</sub>O (1) ITZ (202.7 mg; 0.29 mmol) was dissolved in 25 ml of methanol under heat. Then, a solution of ZnCl<sub>2</sub> (22 mg; 0.16 mmol) in 15 ml of methanol was added dropwise, and the reaction mixture was kept under reflux for 6 h. During this time, there was no change in color. The reaction was then cooled off and the formation of a solid was observed when it reached room temperature. The solution was then filtered and evaporated until dry, and it was washed with abundant water and diethyl ether. The white solid was dried under vacuum. (197 mg) 79% analysis calculated for C<sub>70</sub>H<sub>80</sub>Cl<sub>6</sub>N<sub>16</sub>O<sub>10</sub>Zn, C, 52.79; H, 5.09; N, 14.08. Found: C, 52.82; H, 4.62; N, 13.54%. ESI-MS (*m/z*) [M+H<sup>+</sup>] = 1,547, [MCl] = 1,511 IR (KBr, cm<sup>-1</sup>):  $\nu$  (C=O) 1,701,  $\nu$  (C=N) 1,586,  $\nu$  (C=C) 1,452.  $\Lambda$ (DMSO) (Scm<sup>2</sup>mol<sup>-1</sup>): 4.60. <sup>1</sup>H-NMR (CDCl<sub>3</sub>) [ $\delta$  ppm, (integral, assignation)]: 0.90 (3H, H45), 1.39 (3H, H46), 1.74 (1H, H44), 1.85 (1H, H44'), 3.21 (4H, H27, H31), 3.23 (4H, H28, H30), 3.58 (1H, H18'), 3.82 (2H, H15', H18), 3.89 (1H, H15), 4.29 (1H, H43), 4.35 (1H, H16), 4.80 (2H, H6, H6'), 6.81, (2H, H21, H25), 6.94 (2H, H22, H24), 6.98 (2H, H33, H37), 7.27 (1H, H9), 7.41 (2H, H34, H36), 7.47 (1H, H11), 7.54 (1H, H8), 7.62 (1H, H42), 8.01 (1H, H1), 8.69 (1H, H4). <sup>13</sup>C-NMR (CDCl<sub>3</sub>) [ $\delta$  ppm, (assignation)]: 152.56 (C20), 152.06 (C39), 151.06 (C32), 150.57 (C12), 146.2 (C23), 145.08

**TABLE 5** Anti-*Sporothrix* sp. effect and hemolytic activity of Zn-ITZ-complexes

Compound	Antifungal activity ( $\mu\text{M}$ ) of:				Hemolytic activity ( $\mu\text{M}$ )		
	<i>Sporothrix brasiliensis</i>		<i>Sporothrix schenckii</i>		HA <sub>50</sub> <sup>b</sup>	SI <sup>c</sup> for <i>S. brasiliensis</i>	SI for <i>S. schenckii</i>
	MIC	MFC <sup>a</sup>	MIC	MFC			
ITZ	0.6	>20	1.25	>20	700	1,166.7	560
Zn(ITZ) <sub>2</sub> Cl <sub>2</sub> (1)	0.08	20	0.08	2.5	>1,000	>12,500	>12,500
Zn(ITZ) <sub>2</sub> (OH) <sub>2</sub> (2)	0.3	>20	0.16	>20	ND <sup>d</sup>	ND	ND
ZnCl <sub>2</sub>	>20	>20	>20	>20	>1,000	>50	>50
ZnAc <sub>2</sub> ·2H <sub>2</sub> O	>20	>20	>20	>20	ND	ND	ND

<sup>a</sup>Minimum fungicidal concentration.<sup>b</sup>50% hemolytic concentration.<sup>c</sup>Selective index (SI) = HA<sub>50</sub>/MIC.<sup>d</sup>ND, not determined.

(C10), 136.05 (C1), 133.8 (C42), 133.14 (C4), 131.6 (C4), 129.6 (C2), 127.19 (C3), 125.9 (C6), 123.6 (C5), 118.5 (C35), 116.69 (C34/C36), 115.3 (C22/C24), 107.47 (C33/C37), 74.74 (C15), 67.88 (C18), 67.44 (C16), 53.74 (C8), 52.6 (C43), 50.41 (C27/C31), 49.25 (C28/C30), 28.26 (C44), 19.24 (C46), 10.81 (C45).

Zn(ITZ)<sub>2</sub>(OH)<sub>2</sub>·H<sub>2</sub>O (2) ITZ (300 mg; 0.43 mmol) was dissolved in 35 ml of methanol under heat. Then, Zn(Ac)<sub>2</sub>·2H<sub>2</sub>O (47 mg; 0.22 mmol) was dissolved in 15 ml of methanol. The reaction mixture was kept under reflux for 6 h. During the addition of the salt, no change was observed. The solution was filtered while still hot, and the solvent was evaporated until dry. The white solid was washed with abundant water (25 ml) and then diethyl ether (30 ml). The white solid was dried under vacuum for 4 h. (135.6 mg) 39% analysis calculated For C<sub>70</sub>H<sub>78</sub>Cl<sub>6</sub>N<sub>16</sub>O<sub>10</sub>Zn, C, 54.99; H, 5.10; N, 14.66; Found: C, 55.48; H, 4.49; N, 13.99%. ESI-MS (*m/z*) [M - 2OH]<sup>+</sup> = 1,473 IR (KBr, cm<sup>-1</sup>):  $\nu$  (C=O) 1,702,  $\nu$  (C=N) 1,585,  $\nu$  (C=C) 1,451.  $\Lambda$ (DMSO) (Scm<sup>2</sup>mol<sup>-1</sup>): 2.53. <sup>1</sup>H-NMR (CDCl<sub>3</sub>) [ $\delta$  ppm, (integral, assignment)]: 0.90 (3H, H45), 1.39 (3H, H46), 1.72 (1H, H44), 1.88 (1H, 44'), 3.22 (4H, H27, H31), 3.36 (4H, H28, H30), 3.50 (1H, H18'), 3.81 (2H, H15', H18), 3.91 (1H, H15), 4.30 (1H, H43), 4.37 (1H, H16), 4.80 (2H, H6, H6'), 6.80, (2H, H21, H25), 6.93 (2H, H22, H24), 7.03 (2H, H33, H37), 7.25 (1H, H9), 7.41 (2H, H34, H36), 7.47 (1H, H11), 7.56 (1H, H8), 7.62 (1H, H42), 7.93 (1H, H1), 8.31 (1H, H4). <sup>13</sup>C-NMR (CDCl<sub>3</sub>) [ $\delta$  ppm, (assignment)]: 152.58 (C20), 152.16 (C39), 151.16 (C32), 150.47 (C12), 146.22 (C23), 145.18 (C10), 136.15 (C1), 133.83 (C42), 133.24 (C4), 131.16 (C4), 129.65 (C2), 127.29 (C3), 125.93 (C6), 123.62 (C5), 118.54 (C35), 116.59 (C34/C36), 115.33 (C22/C24), 107.37 (C33/C37), 74.64 (C15), 67.78 (C18), 67.34 (C16), 53.73 (C8), 52.16 (C43), 50.31 (C27/C31), 49.15 (C28/C30), 28.16 (C44), 19.34 (C46), 10.83 (C45).

**Parasites.** The MHOM/BR/75Josefa strain of *L. amazonensis* was isolated in 1975 from a patient with diffuse cutaneous leishmaniasis by Cesar A. Cuba-Cuba (Brasilia University, Brazil) and was provided by the *Leishmania* collection of the Instituto Oswaldo Cruz. It has been maintained via inoculation into the base of BALB/c mice tails. Amastigotes were obtained from mice and transformed into promastigotes that were axenically cultured in Warren's medium supplemented with 10% fetal bovine serum (FBS) at 25°C (41). Tachyzoites of the RH strain expressing red fluorescent protein (RH-RFP; kindly given by Tiago Mineo, Universidade Federal de Uberlândia, Brazil) were maintained *in vitro* by serial passages in cultures of human foreskin fibroblasts (HFF-ATCC). Uninfected and *T. gondii*-infected cultures of HFF were cultivated in Dulbecco's modified Eagle's medium (DMEM) and RPMI 1640 media, respectively, supplemented with 2 mM L-glutamine, penicillin/streptomycin antibiotics, and 2% to 10% FBS, at 37°C and 5% CO<sub>2</sub>. The Y strain (DTU II) of *T. cruzi* was used in this study. Trypomastigotes were obtained from the supernatants of infected LLC-MK<sub>2</sub> culture cells (ATCC CCL-7; American Type Culture Collection, Rockville, MD) grown in RPMI 1640 medium with garamycin (Life BioTechnologies, Grand Island, NY) and 10% fetal bovine serum (Gibco), at 37°C and 5% CO<sub>2</sub>. Subconfluent cultures of LLC-MK<sub>2</sub> cells were infected with 5 × 10<sup>6</sup> trypomastigotes. Free parasites were removed after 24 h, and the cultures were maintained in 10% FBS-RPMI 1640 medium. Five days following infection, free trypomastigote forms were found in the cell supernatants. After 10 days, amastigote forms were observed in the cell supernatants. Epimastigote forms were cultivated in liver infusion tryptose medium as previously described (42), and after 4 days of cultivation, they were collected by centrifugation at 350 × *g*. Resident peritoneal macrophages were obtained from CF1 mice according to the Ethics Committee for Animal Experimentation of the Health Sciences Centre, Universidade Federal do Rio de Janeiro (Brazil) under protocol number IBCCF096/097.

**In vitro antiproliferative effects in *L. amazonensis*.** *L. amazonensis* promastigotes and intracellular amastigotes were treated with itraconazole (ITZ), compound 1, and compound 2, and the susceptibility was evaluated by using parasite proliferation curves. Promastigote cultures were initiated at a cell density of 1 × 10<sup>6</sup> cells/ml. The drugs were added after 24 h of growth, and cell densities were evaluated daily in a Neubauer chamber during 72 h of growth. Promastigotes were also treated with ZnAc<sub>2</sub>·2H<sub>2</sub>O and ZnCl<sub>2</sub>, which are the zinc salts used for the synthesis process. To evaluate the effects of compounds on intracellular amastigotes, macrophages from CF1 mice were infected with infective metacyclic promastigotes of *L. amazonensis* at a macrophage-to-parasite ratio of 1:10 at 35°C and 5% CO<sub>2</sub> for 2 h (29). Different concentrations of inhibitors were added after 24 h of interaction. After 72 h of treatment, the effect was evaluated following experimental protocols previously published (28, 29). The IC<sub>50</sub> was calculated for promastigotes and intracellular amastigotes by fitting the values to a nonlinear curve analysis. The regression analyses were performed with SigmaPlot 10 software.

**In vitro antiproliferative effects in *T. gondii*.** Monolayers of HFF cells in 96-well black, clear flat-bottom plates (Corning Costar) were infected with 5,000 RH-RFP tachyzoites/well resuspended in RPMI 1640 medium without phenol red and supplemented with 2 mM L-glutamine, 100 U/ml penicillin and 100 µg/ml streptomycin antibiotics, and 2% FBS. After 4 h of infection, different concentrations (31.2 to 500 nM) of itraconazole (ITZ), compound 1, and compound 2 were added to infected cultures. Infected cells without drugs were used as a positive control (100% proliferation). After 72 and 96 h of treatment, fluorescence was read from the plate bottom, with excitation and emission wavelengths of 532 nm and 588 nm, respectively, in the SpectraMax M2/M2<sup>e</sup> microplate reader (Molecular Devices). IC<sub>50</sub> calculations were done as described above for *L. amazonensis* experiments.

**In vitro antiproliferative effects in *T. cruzi*.** The susceptibility of *T. cruzi* epimastigotes to itraconazole (ITZ), compound 1, and compound 2 was evaluated using parasite proliferation curves. Epimastigote cultures were initiated at a cell density of  $1.0 \times 10^6$  cells/ml and ITZ, compound 1, and compound 2 were added at different concentrations (1, 3, 5, 10, and 15 µM for both compounds) after 24 h of growth. Cell numbers were evaluated daily in a Neubauer chamber during 96 h of growth. For *T. cruzi* amastigote assays, LLC-MK<sub>2</sub> cells ( $2 \times 10^3$  cells/well) cultivated in 96-well black, clear flat-bottom plates (Corning Costar) were infected with  $2 \times 10^4$  trypomastigotes/well resuspended in RPMI 1640 medium without phenol red and supplemented with 2 mM L-glutamine. Next, cultures were labeled with Hoescht 3342 (5 µg/ml; Thermo Fisher) and wheat germ agglutinin-fluorescein isothiocyanate (WGA-FITC) (1 µg/ml; Thermo Fisher) to label nuclei and the host cell cytoplasm, respectively. Fresh media with different concentrations of ITZ, compound 1, and compound 2 was added daily for 3 days (72 h of treatment). The number of intracellular amastigotes and macrophages (infected or not) were counted by nucleus and kinetoplast staining (macrophages and parasites) with high content analysis equipment (Incell 2000 GE Healthcare) equipped with  $\times 20$  magnification (numerical aperture = 0.45). Images were analyzed using the Incell Investigator software (module organelles). Association indices (the mean number of parasites internalized multiplied by the percentage of infected macrophages divided by the total number of macrophages) were determined and used as a parameter to calculate the percentage of infection for each condition. Infected cells without drugs were used as a positive control (100% proliferation). IC<sub>50</sub> calculations were done as described above for *L. amazonensis* experiments.

**Cell cytotoxicity analysis using MTS/PMS assay.** The effect of ITZ and their Zn-ITZ derivatives against host cells was evaluated by the 3-(4,5-dimethylthiazol-2-yl)-5-(3-carboxymethoxyphenyl)-2-(4-sulfophenyl)-2H-tetrazolium/phenazine methosulfate (MTS/PMS) assay (Promega, Madison, WI, USA). For that, 96-well tissue plates containing peritoneal macrophages, LLC-MK<sub>2</sub>, or monolayers of HFF were treated with different concentrations of ITZ, compound 1, and compound 2 for 72 h and 96 h, respectively. A possible cytotoxic effect of the zinc salts ZnAc<sub>2</sub>·2H<sub>2</sub>O and ZnCl<sub>2</sub> were also evaluated in the murine-immortalized blood macrophages RAW 264.7. At the end of treatment, cells were washed with phosphate-buffered saline (PBS), each well was filled with 100 µl of 10 mM glucose in PBS, and 20 µl of MTS reagent was added. The absorbance was read at 490 nm after 3 h of incubation at 37°C, and cytotoxicity was calculated as the percentage of viable cells versus untreated cells (control). The cytotoxic concentration of 50% (CC<sub>50</sub>) was calculated using the same equation and mathematical conditions used for IC<sub>50</sub>. After that, the selective index (SI) was calculated as the ratio of CC<sub>50</sub>/IC<sub>50</sub>.

**Electron microscopy.** Control and treated promastigotes and epimastigotes were fixed in 2.5% glutaraldehyde in 0.1 M cacodylate buffer (pH 7.2) for 1 h at room temperature. After fixation, cells were washed with 0.1 M cacodylate buffer (pH 7.2) and postfixed in a solution containing 1.25% K<sub>4</sub>[Fe(CN)<sub>6</sub>], 1% OsO<sub>4</sub>, 5 mM CaCl<sub>2</sub>, and 0.1 M cacodylate buffer (pH 7.2) for 30 min. Then, cells were washed again in 0.1 M cacodylate buffer (pH 7.2) and separated for transmission electron microscopy (TEM) and scanning electron microscopy (SEM). Experimental protocols for TEM and SEM were published previously (28, 29).

**Fungal isolates and culture conditions.** The reference isolates *S. brasiliensis* CBS 133021 and *S. schenckii* CBS 132984 were grown in the filamentous form in potato dextrose agar medium at 35°C and 5% CO<sub>2</sub> for 7 days and then converted to the pathogenic (yeast) form in brain heart infusion broth at 36°C, with orbital agitation (150 rpm), for 7 days.

**In vitro antifungal activity in *S. brasiliensis* and *S. schenckii*.** The antifungal activity of Zn-ITZ complexes against *Sporothrix* spp. were evaluated according MIC and minimum fungicidal concentration (MFC) values and compared with those of ITZ, ZnCl<sub>2</sub>, and Zn(Ac)<sub>2</sub>·2H<sub>2</sub>O. MIC was determined using the broth microdilution technique described in Clinical and Laboratory Standards Institute protocols M27-A3 (43), with minor modification for use with *Sporothrix* sp. yeasts. Briefly, serial 2-fold dilutions of compounds were prepared in RPMI 1640 medium [supplemented with 2% glucose and buffered to pH 7.2, with 0.165 M 3-(N-morpholine) propane sulfonic acid] into flat-bottom 96-well microplates to obtain a final concentration ranging from 0.04 to 20 µM. The final concentration of  $0.5 \times 10^5$  to  $1 \times 10^5$  cells/ml of yeasts were treated for 48 h at 35°C in a 5% CO<sub>2</sub> chamber. MIC was defined as the concentration that inhibited  $\geq 80\%$  of fungal growth in relation to untreated fungi, as determined by visual inspection in an inverted microscope and confirmed by spectrophotometric readings at 492 nm, in an EMax Plus plate reader (Molecular Devices). MFC values were determined by visual inspection of fungal growth after drug exposure; after MIC determination, 50-µl aliquots of fungal samples were plated onto drug-free agar medium and incubated at 35°C and 5% CO<sub>2</sub> for 5 days. MFC was the lowest drug concentration that induced no fungal growth.

**Hemolytic activity.** The selectivity of Zn(ITZ)<sub>2</sub>Cl<sub>2</sub> (compound 1) toward *S. brasiliensis* and *S. schenckii* was determined according the concentration that promoted 50% hemolysis (HA<sub>50</sub>) of human red blood cells that was estimated as described previously (10). Selectivity indexes were calculated according to the formula  $SI = HA_{50}/MIC$ . The HA<sub>50</sub> values for ITZ and ZnCl<sub>2</sub> were also determined for comparison with Zn(ITZ)<sub>2</sub>Cl<sub>2</sub>. The hemolytic activity was carried out in accordance with a protocol approved by the Human

Research Ethics Committee of Hospital Universitário Clementino Fraga Filho, UFRJ (protocol number 50765015.5.0000.5257).

**Statistical analysis.** For *L. amazonensis* intracellular amastigotes and *T. gondii* and *T. cruzi* assays, analyses were carried out in GraphPad Prim 8 (CA, USA) using one-way ANOVA, followed by Bonferroni's multiple-comparison test. Besides, for promastigotes, the two-way ANOVA with Dunnett's *post hoc* test was used. Three independent experiments were carried to calculate the mean and standard deviation for each antiproliferative analysis.

## ACKNOWLEDGMENTS

We are grateful to Jonatha Lima for the elemental analysis at INMETRO.

We also acknowledge the Brazilian funding agencies Coordenação de Aperfeiçoamento de Pessoal de Nível Superior (CAPES), Conselho Nacional de Desenvolvimento e Pesquisa (CNPq), and Fundação Carlos Chagas Filho de Amparo à Pesquisa do Estado do Rio de Janeiro (FAPERJ) for financial support.

## REFERENCES

- Barone G, Terenzi A, Lauria A, Almerico AM, Leal JM, Busto N, García B. 2013. DNA-binding of nickel(II), copper(II) and zinc(II) complexes: structure-affinity relationships. *Coord Chem Rev* 257:2848–2862. <https://doi.org/10.1016/j.ccr.2013.02.023>.
- Wee HA, Dyson PJ. 2006. Classical and non-classical ruthenium-based anticancer drugs: towards targeted chemotherapy. *Eur J Inorg Chem* 2006:4003–4018. <https://doi.org/10.1002/ejic.200600723>.
- Busto N, Valladolid J, Aliende C, Jalón FA, Manzano BR, Rodríguez AM, Gaspar JF, Martins C, Biver T, Espino G, Leal JM, García B. 2012. Preparation of organometallic ruthenium-arene-diaminotriazine complexes as binding agents to DNA. *Chem Asian J* 7:788–801. <https://doi.org/10.1002/asia.201100883>.
- Sánchez-Delgado R, Anzellotti A, Suarez L. 2004. Metal complexes as chemotherapeutic agents against tropical diseases: trypanosomiasis, malaria and leishmaniasis. *Mini Rev Med Chem* 4:23–30. <https://doi.org/10.2174/1389557043487493>.
- Navarro M, Gabbiani C, Messori L, Gambino D. 2010. Metal-based drugs for malaria, trypanosomiasis and leishmaniasis: recent achievements and perspectives. *Drug Discov Today* 15:1070–1078. <https://doi.org/10.1016/j.drudis.2010.10.005>.
- Navarro M. 2009. Gold complexes as potential anti-parasitic agents. *Coord Chem Rev* 253:1619–1626. <https://doi.org/10.1016/j.ccr.2008.12.003>.
- Navarro M, Cisneros-Fajardo EJ, Fernandez-Mestre M, Arrieché D, Marchan E. 2003. Synthesis, characterization, DNA binding study and biological activity against *Leishmania mexicana* of  $[\text{Cu}(\text{dppz})_2\text{BF}_4]$ . *J Inorg Biochem* 97:364–369. [https://doi.org/10.1016/S0162-0134\(03\)00290-3](https://doi.org/10.1016/S0162-0134(03)00290-3).
- Navarro M, Visbal G. 2016. Metal-based antiparasitic therapeutics. In Nriagu JO, Skaar EP (ed), *Trace metals and infectious diseases*. MIT Press, London, United Kingdom.
- Colina-Vegas L, Lima Prado Godinho J, Coutinho T, Correa RS, De Souza W, Cola Fernandes Rodrigues J, Batista AA, Navarro M. 2019. Antiparasitic activity and ultrastructural alterations provoked by organoruthenium complexes against: *Leishmania amazonensis*. *New J Chem* 43:1431–1439. <https://doi.org/10.1039/C8NJ04657C>.
- Gagini T, Colina-Vegas L, Villareal W, Borba-Santos LP, De Souza Pereira C, Batista AA, Kneip Fleury M, De Souza W, Rozental S, Costa LAS, Navarro M. 2018. Metal-azole fungistatic drug complexes as anti-Sporothrix spp. agents. *New J Chem* 42:13641–13650. <https://doi.org/10.1039/C8NJ01544A>.
- Ong YC, Roy S, Andrews PC, Gasser G. 2019. Metal compounds against neglected tropical diseases. *Chem Rev* 119:730–796. <https://doi.org/10.1021/acs.chemrev.8b00338>.
- Diaz JRA, Fernández Baldo M, Echeverría G, Baldoni H, Vullo D, Soria DB, Supuran CT, Camí GE. 2016. A substituted sulfonamide and its Co (II), Cu (II), and Zn (II) complexes as potential antifungal agents. *J Enzyme Inhib Med Chem* 31:51–62. <https://doi.org/10.1080/14756366.2016.1187143>.
- Chohan ZH, Arif M, Akhtar MA, Supuran CT. 2006. Metal-based antibacterial and antifungal agents: synthesis, characterization, and in vitro biological evaluation of Co(II), Cu(II), Ni(II), and Zn(II) complexes with amino acid-derived compounds. *Bioinorg Chem Appl* 2006:1–13. <https://doi.org/10.1155/BCA/2006/83131>.
- Castillo KF, Bello-Vieda NJ, Nuñez-Dallos NG, Pastrana HF, Celis AM, Restrepo S, Hurtado JJ, Ávila AG. 2016. Metal complex derivatives ofazole: a study on their synthesis, characterization, and antibacterial and antifungal activities. *J Braz Chem Soc* 27:2334–2347. <https://doi.org/10.5935/0103-5053.20160130>.
- Tapiero H, Tew KD. 2003. Trace elements in human physiology and pathology: zinc and metallothioneins. *Biomed Pharmacother* 57:399–411. [https://doi.org/10.1016/S0753-3322\(03\)00081-7](https://doi.org/10.1016/S0753-3322(03)00081-7).
- Sharquie KE, Najim RA, Farjou IB. 1997. A comparative controlled trial of intralesionally-administered zinc sulphate, hypertonic sodium chloride and pentavalent antimony compound against acute cutaneous leishmaniasis. *Clin Exp Dermatol* 22:169–173. <https://doi.org/10.1111/j.1365-2230.1997.tb01054.x>.
- Brewer GJ. 2001. Zinc acetate for the treatment of Wilson's disease. *Expert Opin Pharmacother* 2:1473–1477. <https://doi.org/10.1517/14656566.2.9.1473>.
- Prasad AS, Fitzgerald JT, Bao B, Beck FW, Chandrasekar PH. 2000. Duration of symptoms and plasma cytokine levels in patients with the common cold treated with zinc acetate: a randomized, double-blind placebo-controlled trial. *Ann Intern Med* 133:245–252. <https://doi.org/10.7326/0003-4819-133-4-200008150-00006>.
- Burza S, Croft SL, Boelaert M. 2018. Leishmaniasis. *Lancet* 10151:951–970. [https://doi.org/10.1016/S0140-6736\(18\)31204-2](https://doi.org/10.1016/S0140-6736(18)31204-2).
- Oryan A, Akbari M. 2016. Worldwide risk factors in leishmaniasis. *Asian Pac J Trop Med* 9:925–932. <https://doi.org/10.1016/j.apjtm.2016.06.021>.
- Barral A, Pedral-Sampaio D, Grimaldi G, Momen H, McMahon-Pratt D, Ribeiro De Jesus A, Almeida R, Badaro R, Barral-Netto M, Carvalho EM, Johnson WD. 1991. Leishmaniasis in Bahia, Brazil: evidence that *Leishmania amazonensis* produces a wide spectrum of clinical disease. *Am J Trop Med Hyg* 44:536–546. <https://doi.org/10.4269/ajtmh.1991.44.536>.
- WHO. 2018. Chagas disease (American trypanosomiasis). WHO, Geneva, Switzerland.
- Soeiro MNC, de Castro SL. 2009. *Trypanosoma cruzi* targets for new chemotherapeutic approaches. *Expert Opin Ther Targets* 1:105–121. <https://doi.org/10.1517/14728220802623881>.
- Queiroz-Telles F, Fahal AH, Falci DR, Caceres DH, Chiller T, Pasqualotto AC. 2017. Neglected endemic mycoses. *Lancet Infect Dis* 17:e367–e377. [https://doi.org/10.1016/S1473-3099\(17\)30306-7](https://doi.org/10.1016/S1473-3099(17)30306-7).
- Orofino-Costa R, Rodrigues AM, de Macedo PM, Bernardes-Engemann AR. 2017. Sporotrichosis: an update on epidemiology, etiopathogenesis, laboratory and clinical therapeutics. *An Bras Dermatol* 92:606–620. <https://doi.org/10.1590/abd1806-4841.2017279>.
- Rodrigues JCF, Godinho JLP, de Souza W. 2014. Biology of human pathogenic trypanosomatids: epidemiology, lifecycle and ultrastructure, p 1–42. In Santos A, Branquinho M, d'Ávila-Levy C, Kneipp L, Sodré C (ed), *Proteins and proteomics of leishmania and trypanosoma*. Subcellular biochemistry, vol 74. Springer, Dordrecht, The Netherlands.
- Mahajan VK. 2014. Sporotrichosis: an overview and therapeutic options. *Dermatol Res Pract* 2014:272376–272313. <https://doi.org/10.1155/2014/272376>.
- de Macedo-Silva ST, Visbal G, Urbina JA, de Souza W, Rodrigues J. 2015. Potent in vitro antiproliferative synergism of combinations of ergosterol biosynthesis inhibitors against *Leishmania amazonensis*. *Antimicrob Agents Chemother* 10:6402–6418. <https://doi.org/10.1128/AAC.01150-15>.
- De Macedo-Silva ST, Urbina JA, De Souza W, Rodrigues J. 2013. In vitro

- activity of the antifungal azoles itraconazole and posaconazole against *Leishmania amazonensis*. *PLoS One* 8:e83247. <https://doi.org/10.1371/journal.pone.0083247>.
30. Martins TAF, Diniz LDF, Mazzeti AL, Do Nascimento Á, Caldas S, Caldas IS, De Andrade IM, Ribeiro I, Bahia MT. 2015. Benznidazole/itraconazole combination treatment enhances anti-*Trypanosoma cruzi* activity in experimental Chagas disease. *PLoS One* 10:1–12. <https://doi.org/10.1371/journal.pone.0128707>.
  31. Martins-Duarte ÉDS, De Souza W, Vommaro RC. 2008. Itraconazole affects *Toxoplasma gondii* endodyogeny. *FEMS Microbiol Lett* 2:290–298. <https://doi.org/10.1111/j.1574-6968.2008.01130.x>.
  32. Martins-Duarte ÉS, Lemgruber L, de Souza W, Vommaro RC. 2010. *Toxoplasma gondii*: fluconazole and itraconazole activity against toxoplasmosis in a murine model. *Exp Parasitol* 24:466–469. <https://doi.org/10.1016/j.exppara.2009.12.011>.
  33. Wang Y, Li Y, Zhou Z, Zu X, Deng Y. 2011. Evolution of the zinc compound nanostructures in zinc acetate single-source solution. *J Nanopart Res* 13:5193–5202. <https://doi.org/10.1007/s11051-011-0504-y>.
  34. Gattorno GR, Oskam G. 2006. Forced hydrolysis vs self-hydrolysis of zinc acetate in ethanol and iso-butanol. *ECS Trans* 3:23–28. <https://doi.org/10.1149/1.2357093>.
  35. Sharma S, Ramani J, Bhalodia J, Patel N, Thakkar K. 2011. Synthesis, characterization and antimicrobial activity of some transition metal complexes (Mn, Co, Zn, Ni) with L-proline and Kojic acid. *Adv App Sci Res* 2:374–382.
  36. Dudev T, Lim C. 2000. Tetrahedral vs octahedral zinc complexes with ligands of biological interest: a DFT/CDM study. *J Am Chem Soc* 122: 11146–11153. <https://doi.org/10.1021/ja0010296>.
  37. Geary WJ. 1971. The use of conductivity measurements in organic solvents for the characterisation of coordination compounds. *Coord Chem Rev* 1:81–122. [https://doi.org/10.1016/S0010-8545\(00\)80009-0](https://doi.org/10.1016/S0010-8545(00)80009-0).
  38. Bossche HV, Marichal P, Le Jeune L, Coene MC, Gorrens J, Cools W. 1993. Effects of itraconazole on cytochrome P-450-dependent sterol 14 $\alpha$ -demethylation and reduction of 3-ketosteroids in *Cryptococcus neoformans*. *Antimicrob Agents Chemother* 37:2101–2105. <https://doi.org/10.1128/aac.37.10.2101>.
  39. Krężel A, Maret W. 2016. The biological inorganic chemistry of zinc ions. *Arch Biochem Biophys* 611:3–19. <https://doi.org/10.1016/j.abb.2016.04.010>.
  40. Reddy A, Sangenito LS, Guedes ADA, Branquinho MH, Kavanagh K, McGinley J, Dos Santos ALS, Velasco-Torrijos T. 2017. Glycosylated metal chelators as anti-parasitic agents with tunable selectivity. *Dalton Trans* 46:5297–5307. <https://doi.org/10.1039/c6dt04615k>.
  41. Warren LG. 1960. Metabolism of *Schizotrypanum cruzi* Chagas. I. Effect of culture age and substrate concentration on respiratory rate. *J Parasitol* 46:529–539. <https://doi.org/10.2307/3274932>.
  42. Camargo E. 1964. Growth and differentiation in *Trypanosoma cruzi*. *Rev Inst Med Trop Sao Paulo* 6:93–100.
  43. Clinical and Laboratory Standards Institute. 2012. M27-S4 reference method for broth dilution antifungal susceptibility testing of yeasts, fourth informational supplement. Clinical and Laboratory Standards Institute, Wayne, PA.